Proceedings World Geothermal Congress 2010
Bali, Indonesia, 25-29 April 2010

Use of MT3DMS for Heat Transport Simulation of Shallow Geothermal Systems

Jozsef Hecht-Méndez, Nelson Molina-Giraldo, Philipp Blum and Peter Bayer

University of Tübingen, Center for Applied Geoscience (ZAG), Sigwartstrasse 10, 72076, Tübingen, Germany

jozsef.hecht-mendez@uni-tuebingen.de

Keywords: Geothermal systems; Heat transport simulation; Convection; Borehole heat exchanger.

ABSTRACT

The multi-species transport model MT3DMS is applied to simulate heat transport in shallow confined aquifers. This is done by taking advantage of the mathematical similarities between the description of heat and solute transport. A comprehensive analysis on the applicability of MT3DMS (version 5.2) for heat transport simulation of closed shallow geothermal systems is shown. MT3DMS simulations are compared with results from heat analytical solutions and with those from the established numerical code FEFLOW. Issues regarding the definition of the boundary conditions, as well as the evaluation of the type of the numerical advection solver are investigated. The computed results are examined based on residual errors. The overall agreement of MT3DMS with the analytical solutions and FEFLOW is good. Larger discrepancies are only found close to the heat source, which is due to the inherent differences of the numerical methods used by each code and the boundary conditions required by the analytical solutions. Despite these differences we find that MT3DMS can be successfully applied to simulate heat transport in saturated and confined porous media under the influence of GSHP systems.

1. INTRODUCTION

During the last decade, direct applications of shallow geothermal energy for heating and cooling of houses and facilities have shown a constant increase (Sanner et al. 2003, Lund et al. 2005). By 2005, the annual growth rate of these technologies was estimated to be 7.5 % (Lund et al. 2005). Particularly in Germany, from 2005 to 2006 the number of shallow geothermal installations has more than doubled (44,000 ground source heat pump systems in 2006, Hähnlein et al. 2008). Consequently, the density of installations of such systems in residential and industrial areas is steadily growing. Besides important questions associated with heat extraction rights, issues related to changes in the aquifer ambient temperature due to the presence of these systems are of concern (Ferguson 2009). Therefore reliable prediction of the performance of such systems is essential. An important factor is the groundwater flow regime. On the one hand, it has been proven that the groundwater flow enhances heat transfer from the material surrounding a borehole heat exchanger (BHE), and on the other hand, for high-flow regimes the temperature changes in the aquifer are diminished in comparison to no-flow conditions, i.e. only heat conduction.

An appealing way to evaluate together the last two aspects is using numerical models, and in particular for planning of larger ground source heat pump (GSHP) systems with multiple potentially interacting BHEs such models are commonly applied. Many of these codes rely on heat conduction and, therefore, heat convection is not simulated (e.g. EED, TRNSYS, DST, SBM). Among others, Eskilson (1987), Chiasson et al. (2000), Gelhin and Hellström (2003), Diao et al. (2004), Fujii et al. (2005), Fan et al. (2007) and Guimera et al. (2007) have investigated the effect of groundwater flow in such low enthalpy systems. In all of these studies, numerical simulation is a key tool, generally contrasted with analytical solutions and/or experimental data. Some of the codes used in these investigations are developed as part of the study (as in Diao et al. 2004 and Fan et al. 2007) and some are commercial, e.g. FEFLOW (Diersch, 2002).

In this study we apply the well-known solute transport numerical code MT3DMS (version 5.2, Zheng and Wang 1999) for simulating heat transport of closed-loop GSHP systems. MT3DMS is a finite difference code with almost 20 years of continuous development. It is public domain, open source, widely tested for a variety of solute transport problems and integrates five different solvers for the advection term (i.e. convection term for heat transport). In the following we exploit the mathematical similarities between solute and heat transport. The conforming coefficients of the solute equations are reformulated for simulating temperature changes, and accordingly the thermal input parameters are defined. The main objective is to examine the applicability of the solute transport code for simulations of heat transport due to changes in temperature exerted by a single closed-loop GHSP system. This is done by comparing MT3DMS simulations with results obtained by analytical solutions and alternative numerical methods such as FEFLOW.

2. MATHEMATICAL DESCRIPTION

In this chapter, mathematical descriptions of heat and solute transport, as well as the coefficient reformulations, are presented. The following Equation 1 represents the partial differential equation describing solute transport in transient groundwater flow systems solved by MT3DMS:

$$\left(1+\frac{\rho_b K_d}{n}\right)\frac{\partial C}{\partial t} = div\left[(D_m + \alpha v_a)gradC\right] - div(v_a C) + \frac{q_k C}{n} \qquad (1)$$

The term on the left side denotes the ratio between the total solute concentration (C) and the mobile solute concentration given by the distribution coefficient K_d (ρ_b and n are the bulk density of the solid and the porosity, respectively). The first term in the right side is the hydrodynamic dispersion term, including pure molecular diffusion (D_m) and mechanical dispersion ($\alpha\ v_a$). The latter comprises longitudinal dispersivity (α) and groundwater velocity (v_a). The second term describes solute advection and the third term ($q_k\ C$) represents the mass entering or leaving the domain or the source and sink with unit of Kg m^{-3} s^{-1}.

In comparison, heat transport is described in Equation 2, following the principle of heat conservation, including conduction and convection (de Marsily 1986):

$$\left(\frac{\rho_m c_m}{n\rho_w c_w}\right)\frac{\partial T}{\partial t} = div\left[\left(\frac{\lambda_m}{n\rho_w c_w} + \alpha v_a\right)gradT\right] - div(v_a T) + \frac{q_h}{n\rho_w c_w} \qquad (2)$$

Here, as is common, thermal equilibrium between the phases (groundwater and aquifer matrix) is assumed, where $\rho_m c_m$ (volumetric heat capacity of the porous media) is computed as the weighted arithmetic mean of solid rock and pore fluid heat capacities. In the first term on the right side, the ratio between the thermal conductivity λ_m of the porous media and the volumetric heat capacity of the fluid ($\rho_w c_w$) and the porosity n, represents thermal diffusion (D_h), which is analogous to molecular diffusion. The remainder term corresponds to mechanical dispersion ($\alpha\ v_a$). The second term on the right side represents thermal convection (analogous to solute advection). The last term is the expression of the source and sinks terms. Here the parameter q_h represents the energy input or extraction (which can be expressed as Watts or J s^{-1}).

2.1 Coefficients Reformulation

In order to use MT3DMS for heat transport simulation, the coefficients in Equations 1 and 2 have to be correlated. By doing this, the standard (solute transport related) input parameters given for the code can then be expressed in terms of thermal parameters.

Table 1 lists the input parameters after reformulation of each term, the parameter units, and the input packages of MT3DMS where the parameter values are entered. The first and second input parameters (distribution coefficient and molecular diffusion) are now expressed as thermal coefficients. For the dispersivity coefficient (third parameter in the table) no reformulation is necessary, assuming that the hydraulic and thermal dispersion is the same. For the last input parameter, in order to be consistent with the dimensions relating contaminant with heat transport, the units of concentration [kg m^{-3}] must be equivalent to the unit Kelvin [K]. Thus energy input/extraction is stated similar to a mass load per unit volume of aquifer.

Table 1: Resulting MT3DMS input parameter after coefficient correlation of the solute and heat transport equations.

Input parameter	Units	MT3DMS package
$K_d = \frac{c_s}{\rho_w c_w}$	[$m^3\,kg^{-1}$]	Chemical reaction
$D_m = \frac{\lambda_m}{\rho_w c_w}$	[$m^2 s^{-1}$]	Dispersion
$\alpha = \alpha$	[m]	Dispersion
$q_k C = \frac{q_h}{\rho_w c_w}$	[K s^{-1}]	Sink and source mixing

2.2 Assumptions for Code Application

Some assumptions for using the code are made. The temperature dependencies of some parameters such as of density and viscosity of the moving water as well as of thermal conductivity and heat capacity of water and matrix are neglected. The errors introduced by these simplifications are expected to be highest in the vicinity of the BHEs, where the temperature changes are maximal. However, since usually shallow geothermal applications operate within a temperature range of only few degrees, these errors still seem acceptable.

3. METHODOLOGY

The procedure followed in this study comprises two parts. In the first part, issues related to the conceptualization of the model are discussed. Furthermore, the efficiencies of different numerical advection solvers included in MT3DMS are investigated.

At this stage the following analyses are carried out:

- Model domain size analysis;
- Size adjustment of the cell where energy is extracted (source cell) to the real dimensions of a BHE;
- Evaluation of the various advection solvers included in MT3DMS for three different convective scenarios.

The second part is dedicated to comparing simulated results with analytical solutions for 2D- and 3D-cases. MT3DMS results are also contrasted with numerical results obtained by the finite element code FEFLOW for the same scenarios.

The transport code MT3DMS alone does not compute the flow field, i.e. the numerical solution for groundwater flow for a specific domain, boundary and initial conditions. As a preprocessor, a groundwater flow simulator must be used. Commonly, the USGS routine MODFLOW (Harbaugh et al. 2000) is selected. It is fully compatible with the solute transport code MT3DMS and includes an output format that interfaces with it. For both of the codes, the same model domain size and spatial discretization have to be defined. In this work a forced groundwater flow is generated by assigning two fixed hydraulic heads (constant head boundary conditions) at the east and west borders with different values. No flow conditions are set at the north and south borders (Figure 1).

We devise a set of different hypothetical scenarios that are used as reference case studies for the analyses. These scenarios are distinguished according to the underlying Péclet number (*Pe*). The non-dimensional *Pe* denotes the ratio between the heat transported by fluid motion and the heat transported by convection, i.e. the higher the *Pe* the more convective the systems. It is expressed as

$$Pe = \frac{q l \rho_w C_w}{\lambda_m} \tag{3}$$

where λ_m is the thermal conductivity of the porous media. It is computed as the weighted average of the thermal conductivity of water and solids. Parameter q represents the Darcy velocity and l is the characteristic length (in this work the predominant grid size of the finite differences mesh). Both two-dimensional (2D) and three-dimensional (3D) models are set up.

3.1 Model and Scenario Settings

3.1.1 Scenario Set-Up for Model Conceptualization Issues and Examination of Advection Solvers

An isotropic model with one BHE is used with uniform hydraulic conductivity ($K = 8 \times 10^{-3}$ m s^{-1}) and 26 % porosity. A uniform cell size of 1 m is used in each analysis. A convective scenario with $Pe = 7$ is set for the domain size analysis and for studying various discretizations at the source cell. The model domain dimensions are first evaluated using various sizes, ranging from 100 m × 100 m to 1000 m × 1000 m. Subsequently, the domain size is fixed and the source cell size is investigated. The size of the source is decreased from 10 m × 10 m to 0.15 m × 0.15 m.

An initial temperature of T_o = 285.15 K is assigned to the entire domain. Constant thermal boundary conditions (Dirichlet) are applied only at the west boundary. At the

north and south boundaries, thermal flows are avoided. At the BHE source cell, a continuous energy extraction of 60 W m^{-1} is set. This value is based on typical reference values from the German Engineer Association guidelines for thermal use of the underground (VDI 2001). Table 2 lists parameters entered in the transport model.

Table 2: Input parameters for MT3DMS

Symbol	Variable	Value	Unit	MT3DMS package
n	porosity	0.26	-	BTN
λ_m	thermal conductivity of the porous	2.0	W m^{-1} K^{-1}	-
$\rho_w c_w$	volumetric heat capacity of the water	$4.2 \cdot 10^6$	J $m^{-3}K^{-1}$	-
ρ_s	density of the solid material	2650	kg m^{-3}	-
c_s	specific heat capacity of the solid	880	J $kg^{-1}K^{-1}$	-
ρ_b	dry bulk density	1961	kg m^{-3}	RCT
K_d	partition coefficient	$2.2 \cdot 10^{-4}$	m^3 kg^{-1}	RCT
α_l	longitudinal dispersivity	0.5	m	DSP
α_{th}	transversal horizontal	0.05	m	DSP
α_{tv}	transversal vertical	0.05	m	DSP
D_h	thermal diffusivity	$1.9 \cdot 10^{-6}$	m^2s^{-1}	DSP
T_u	undisturbed ground temperature	285.15	K	BTN
R	retardation factor	2.59	-	RCT

Using the same hydraulic conductivity and the same porosity, three convective scenarios are generated with different *Pe* (*Pe* = 1, 7, and 20) for investigating the available advection solvers in MT3DMS. Hence, simulations for each scenario are performed using the five advection solver options. These solvers are: standard finite difference (FD), method of characteristics (MOC), modified method of characteristics (MMOC), hybrid method of characteristics (HMOC) and the third order total variation diminishing (ULTIMATE). Each of them has advantages and disadvantages from the mathematical point of view. Here, without further discussion, we only focus on their accuracy and efficiency in terms of computational running time.

3.1.2 Scenario Set Up for the Comparison with Analytical and Alternative Numerical Results

In this next part of the analysis, only one scenario is used with a Darcy velocity of 0.83 m d^{-1} and a grid size of 0.5 m. The *Pe* for this scenario is 10, which indicates a convection-dominated system.

The base model spans a 300 m × 200 m domain with regular grid spacing ($\Delta x = \Delta y = 0.5$ m). The same conceptualization as shown in Figure 1 is used. One BHE is represented by one source cell for the 2D case and three vertically adjacent cells for the 3D cases, where energy is extracted. At the BHE, the mesh is locally refined to 0.15 m × 0.15 m (a telescopic refinement from 0.5 m to 0.15 m is applied). Vertical heat transfer is ignored for the 2D cases and only considered in the 3D simulations. For the latter, a model with 13 uniform one-meter layers of same horizontal domain size is set up.

The BHE for the 3D scenarios is represented as planar source by three adjacent cells, aligned in the vertical direction. Same initial conditions (T_o = 285.15 K) and boundary conditions as for the previous analysis are used. Also the same energy extraction value (60 W m^{-1}) is applied at the source cell. Additional thermal model parameters are listed in Table 2.

The third-order TVD (ULTIMATE) scheme is used for solving the advection term while the *Generalized Conjugate Gradient* (GCG) solver is employed for the non-advective terms. In order to fulfill the stability criteria related to the third-order TVD scheme, automatic time step estimation is selected.

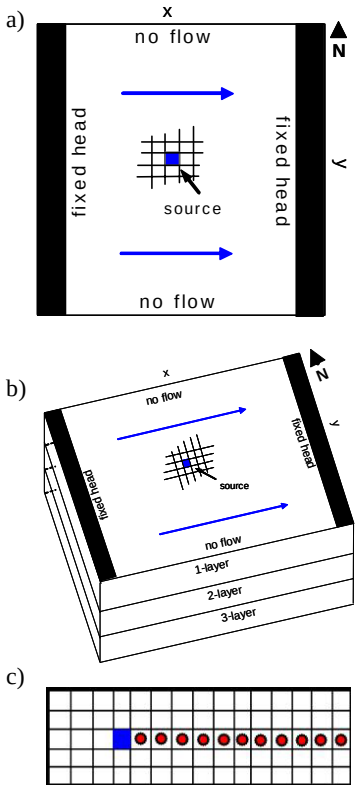

Figure 1: Schemes of model set-up and hypothetical scenarios: a) 2D scenarios with groundwater flow direction (blue arrows), b) 3D scenarios and c) sketch of the source (blue square) and the observation points (red circles).

For the FEFLOW model set-up a triangular mesh is selected with elements of about 1 m size. Same groundwater flow regime and type of boundary and initial conditions are applied to this model. We also use the same input parameter settings as for MT3DMS (Table 2). A fundamental difference between both codes is the definition of the source. In MT3DMS, the energy extraction is assigned to a cell and therefore it is related to its volume. In FEFLOW, for the 2D case the energy extraction is assigned on one node aligned on the mesh. For the 3D case, the energy extraction is also exerted in one node which extends vertically (here 3 m).

However, we computed energy extraction values that correspond to equal realized energy extraction (60 W m^{-1}) in both codes.

In this second part of the investigation, MT3DMS is examined as follows: 1) MT3DMS results are compared with results from analytical solutions As in analytical methods, the line source model by Diao et al. (2004) is used for comparing the 2D results. The planar source solution by Domenico and Robbins (1985) is considered for the 3D scenarios. Both analytical solutions are suitable for simulation of continuous heat sources. 2) MT3DMS results are contrasted with numerical results from FEFLOW (version 5.2, Diersch 2002). This well-established code has already been used for heat transport simulations of shallow geothermal systems in various applications (Nam et al. 2008, Rühaak et al. 2008, Kupfersberger 2009).

Simulations with different modeling concepts and codes are compared at observations points in the model that are located at and downgradient of the source (Figure 1c). The differences in predicted temperature values between the individual methods are quantified by using the method of efficiencies (Loague and Green 1991).

4. RESULTS AND DISCUSSION

4.1 MT3DMS Mesh Set-Up

First, the results from analyzing the effect from different model domain sizes (2D case) are presented. Figure 2 shows the simulations for various model domain sizes (m × m) compared with the predictions by the 2D analytical solution. For the smallest grid size (100 m × 100 m), the curve of the numerical results does not agree with the analytical solution curve. This is due to the significant influence of the boundaries on the numerical results. For more distant boundaries and grid sizes ranging from 200 m × 200 m to 500 m × 500 m, the agreement between the curves is good, in particular at distance from the source larger than 2 m. The difference of about 0.25 K near the source is due to simulated upgradient energy losses. These occur due to the uniform definition of the thermal diffusivity D_h and the longitudinal dispersivity α_l.

For domain sizes larger than 500 m × 500 m, the curves of the simulated results get slightly farther away from the analytical solution, for instance, for 700 × 700 m, the temperature difference reaches up to 0.3 K. It is possible that for these large domain sizes, a regional component or increased numerical inaccuracy for the larger number of cells is influencing the simulated results, causing a smoothing out of the temperature change due to the energy extracted from the aquifer. This situation leads to a deviation of the numerical results from the analytical solution. Although not shown, similar results are obtained for 3D models.

When analyzing the role of the source cell size (and the refinement at the source cell), it is found that the smaller the source cell size the better the agreement between numerical and analytical results (Figure 3).

For source cell sizes of 3 m, 5 m and 10 m, the location of the first observation point is 2 m, 3 m and 5.5 m, respectively. As a result, the starting points of the simulated curves are different. As can be extracted from Figure 3, the best agreement is found for a minimum source cell size of 0.15 m × 0.15 m. This confirms theory: the smaller the source cell size in the numerical model the closer we are to representing the infinitesimal source defined in the analytical solution. However, in practice an exact numerical representation of the infinitesimal condition of the analytical source with an infinitesimal cell size is impossible. Aside from this, please note that as the sizes are diminished at the source cell, the computational time considerably increased.

4.2 Role of Numerical Solver

Three different scenarios are used for analyzing the five advection solvers included in MT3DMS. A model with 500 m × 500 m size and a uniform grid cell of 1 m is set up for all scenarios. The fundamental difference is the groundwater flow velocity. Three values of *Pe* are applied: 1, 7 and 20.

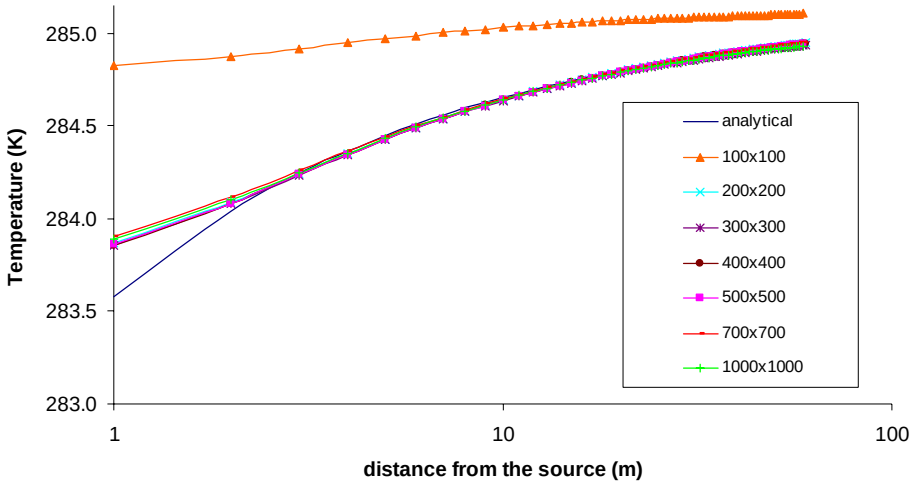

Figure 2: Comparison of the 2D numerical results with the analytical solution for various model domains in m × m (x-axis in logarithmic scale).

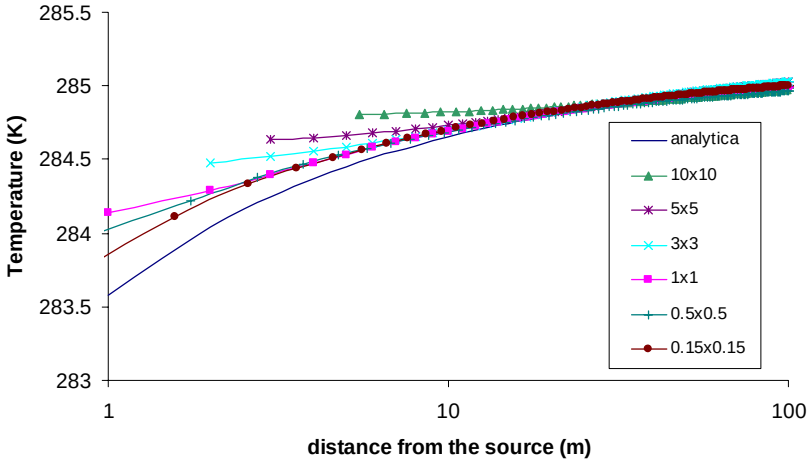

Figure 3: Comparison between the 2D numerical and analytical solution for various source cell sizes in m × m (x-axis in logarithmic scale).

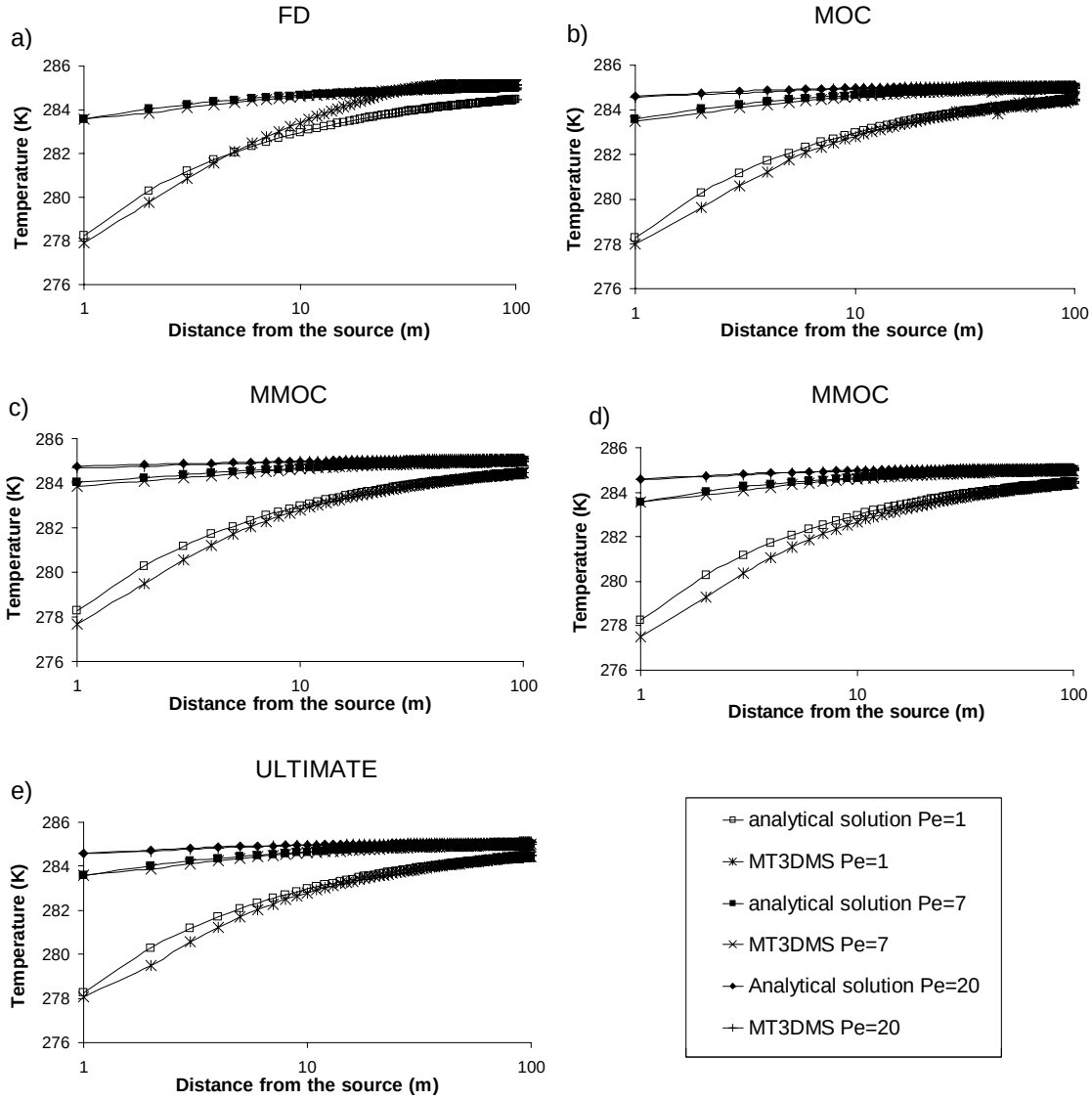

Figure 4: Comparison between numerical and analytical results for three values of *Pe* applying the five advection solver methods included in MT3DMS: a) Finite differences (FD), b) Method of characteristics (MOC), c) Modified method of characteristics (MMOC), d) Hybrid method of characteristics (HMOC), and e) Third order TVD (ULTIMATE).

Table 3 lists required computational times for the various solvers and scenarios, and Figure 4 shows the comparison between numerical and analytical results. The simulations were performed with a personal computer with AMD Sempron 3000+ processor of 2.0 GHz and 1 Gb RAM. The fastest solver is the FD with the shortest running time for each scenario. Nevertheless, its accuracy diminishes when incrementing the flow velocities. Even for the highest *Pe* this solver does not converge. The solvers based on particle tackling techniques (MOC, MMOC and HMOC) need more running time to finish the simulation. Their performance is satisfactory for the whole range of *Pe*. Nevertheless, when using these solvers, special care must be done in selecting the number of particles used within the simulation. A low number of particles will not lead to convergence of the solver and an overestimated number will increase the computational time. The ULTIMATE solver has the longest running time for all scenarios. However, its accuracy is the highest for all test cases. An advantage of using this solver is that it is not needed to set specific solver parameters. Taking the agreement between numerical and analytical results as criterion, the ULTIMATE solver is suited best and thus selected for the subsequent second part of the investigation.

Table 3: Computational time for each advection solver

Pe	Time (min)				
	HMOC	FD	MOC	MMOC	ULTIMATE
1	1.8	1.3	1.8	1.8	2.5
7	9.9	4.0	10.0	9.7	13.0
20	27.3	n/a	27.4	26.8	34.1

Of special interest is the effect of varying the flow regime. As depicted in Figure 4, for the lowest *Pe* (*Pe* = 1), or for the low-flow velocities, the largest temperature change is observed (at 1 m distance from the source), decreasing down to around 278 K (ΔT = 7 K, approximately). As the *Pe* is increased, the disturbance of at the same position diminishes to 283.8 K for *Pe* = 7 and to 284.7 K for *Pe* = 10. Since the moving groundwater carries a constant ambient temperature, the groundwater flow apparently acts as an additional energy supplier for the geothermal system.

This situation prevents the evolvement of larger temperature changes in the surroundings of the BHE. This has also been observed in previous studies focusing on the role of groundwater flow (Chiasson et al. 2000, Fujii et al. 2005, Fan et al. 2007).

4.3 Comparison of Numerical and Analytical Methods

First, the findings for the 2D case are discussed. Figure 5 compares the numerical and analytical results on linear and logarithmic scales. Both perspectives indicate a good agreement between the three curves. This is also quantified by the computed efficiency of 0.96 (1.0 is a perfect agreement) when comparing MT3DMS simulations with those by the analytical solution and by FEFLOW. Only slight differences are found close to the source (< 5 m). As discussed in the previous chapter (see Figure 3), these are due to the grid size at the source cell. While the analytical solution considers an infinitesimal line source, in MT3DMS the source is defined for a cell. The smaller the source cell size, the better the fit between numerical and analytical results. However, with an efficiency of 0.96 the selected source cell size of (0.15 m) appears sufficiently small.

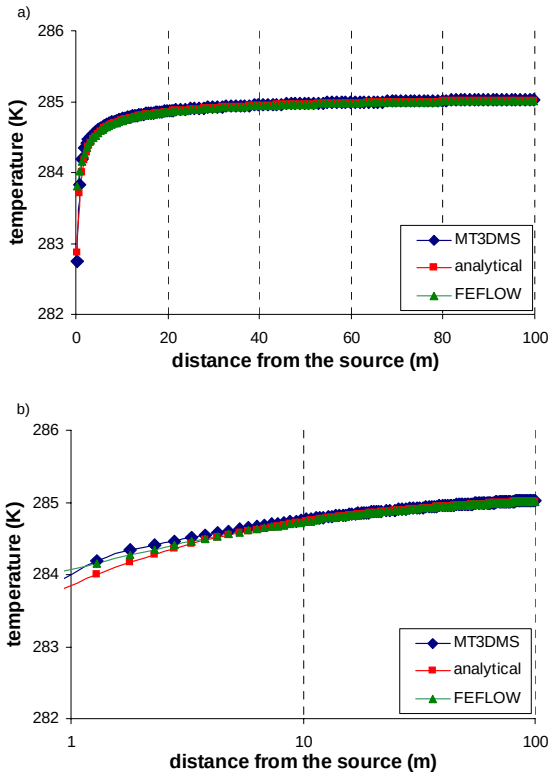

Figure 5: Comparison between the 2D numerical and analytical solution results, a) linear and b) logarithmic scale

For the 3D case satisfactory results are also obtained (Figure 6). The computed efficiencies are 0.98 and 0.7 for the analytical and the FEFLOW results, respectively. The discrepancy with the FEFLOW results is most likely due to the dissimilar source definition used in each numerical code. Remember that the source in MT3DMS is defined as a plane, which is perpendicular to the groundwater flow direction while in FEFLOW it is defined as a node spanned along three layers. Since the source in this case is bigger in the implementation in MT3DMS, the local temperature disturbance in the aquifer is also larger. For instance, in Figure 5a, the temperature close to the source (0.3 m distance from the source), reaches down to 283.7 K. For the same distance in the 3D case, the temperature difference is 282.3 K (Figure 6a).

5. CONCLUSIONS

This scenario-based study demonstrates the applicability of the solute transport code MT3DMS for simulation of heat transport in confined saturated aquifers due to temperature differences exerted by GSHP systems. In MT3DMS a few solute transport coefficients in the mathematical formulation of the code are identified, compared and transformed into those describing heat transport. In principle, this procedure can also be applied to any solute transport code.

For the set-up of a numerical model for heat transport it is important to set the boundary conditions at some prudent distance from the location(s) of the energy extraction. This must be done in order to avoid border effects. However, very large model domains not only increase the computational running time but can slightly worsen numerical results. Of course, model conceptualization has to be adjusted to a specific problem. In this work, a simple homogeneous case

with only one borehole heat exchanger (BHE) was considered.

The study on appropriate source (e.g. BHE) cell size revealed that MT3DMS can effectively represent the dimension of a typical BHE and yield satisfactory results. Different advection solvers can be chosen. Depending on the groundwater velocity one or more of the existing five solver options can yield good results. However, a good balance of solver-specific computational time and desired accuracy certainly depends on each site-specific situation.

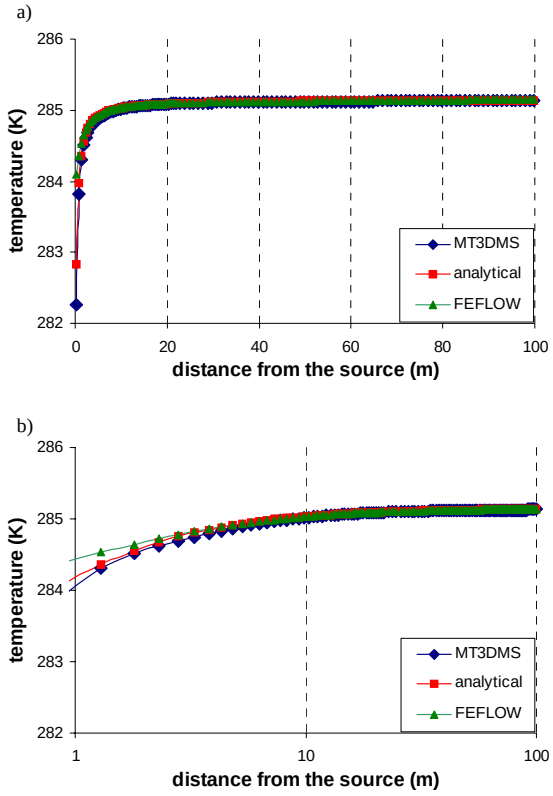

Figure 6: Comparison between the 2D numerical and analytical solution results, a) linear and b) logarithmic scale

The comparisons of MT3DMS with the analytical solutions for the selected 2D and 3D scenarios yield high model efficiencies, 0.96 and 0.98 for each case. These results are encouraging and indicate that the code can reliably represent the thermal effects of the BHE in aquifers. Compared to the established finite difference code FEFLOW, satisfactory results are also obtained, represented in efficiency values of 0.96 and 0.7 for 2D and 3D cases, respectively. Based on these results, numerical simulations of shallow geothermal systems such as GSHP systems including the effects of groundwater flow can successfully be achieved.

REFERENCES

Chiasson, A.D., S.J. Rees and Spitler, J.D.: A preliminary assessment of the effects of ground water flow on closed-loop ground-source heat pump systems. *ASHRAE Transactions*, **106**, (2000), 380-393.

de Marsily, G.: Quantitative Hydrogeology. Orlando: Academic Press, (1986).

Diao, N, Q. Li, and Zhaohong, F.: Heat transfer in ground heat exchangers with groundwater advection. *International Journal of Thermal Sciences*, **43**, (2004), 1203-1211.

Diersch, H.J.G.: FEFLOW 5- User's Manual. Berlin: WASY GmbH, (2002).

Domenico, P.A., and Schwartz F.W.: Physical and Chemical Hydrogeology, 2nd ed. New York: John Wiley & Sons Inc., (1990).

Eskilson, P. Thermal analysis of heat extraction boreholes. *Ph.D. diss*., Department of Mathematical Physics, Lund Institute of Technology, (1987).

Fan, R., Y. Jiang, Y. Yao and Ma, Z.: Theoretical study on the performance of an integrated ground-source heat pump system in a whole year. *Energy*, **32**, (2007), 2199-2209.

Fujii, H. Itoi, R., Fujii, J. and Uchida Y.: Optimizing the design of large-scale ground-coupled heat pump systems using groundwater and heat transport modeling. *Geothermics*, **34**, (2005), 347-364.

Ferguson, G.: Unfinished business in geothermal energy. Ground Water. **47**, (2009), 167-167.

Gehlin, S.E.A. and Hellström, G.: Influence on thermal response test by groundwater flow in vertical fracturesin hard rock. *Renewable* Energy, **28**, (2003), 2221–2238.

Guimera, J., F. Ortuño, E. Ruiz, A. Delos, and Pérez-Paricio, A.: Influence of ground-source heat pumps on groundwater. *Proceedings*, European Geothermal Congress. Unterhaching (2007).

Harbaugh, A.W., E.R. Banta, M.C. Hill, and McDonald, M.G.: MODFLOW-2000, the U.S. Geological Survey modular ground water model, user guide to modularization concepts and the ground water flow process. USGS Open-File Report 00-92, (2000).

Hähnlein, S., P. Grathwohl, P. Bayer, and Blum P.: Cold plumes of ground source heat pumps: Their length and legal situation. *Geophysical Research Abstracts*, **10**, EGU2008-A-07946 (2008).

Kupfersberger, H.: Application of groundwater heat transfer modeling to a regional aquifer in Austria. *Environmental Geology* (accepted), (2009).

Loague, K., and Green R.E.: Statistical and graphical methods for evaluating solute transport models: Overview and application, *Journal of Contaminant Hydrology*, **7**, (1991), 51-73.

Lund, J.W., D.H. Freeston, and Boyd T.L.: Direct Application of geothermal energy: 2005 worldwide review. *Geothermics*, **34**, (2005), 691-727.

Nam, Y., R. Ookaa, and Hwanga S.: Development of a numerical model to predict heat exchange rates for a ground-source heat pump system. *Energy and Buildings*, **40**, (2008), 2133–2140.

Rühaak, W., P. Schätzl, A. Renz, and Diersch H.J.G.: Numerical modeling of geothermal processes: issues and examples. *10th International Mine Water Association Congress, Mine Water and the Environment*. Karlovy Vary, (2008).

Sanner, B., C. Karytsas, D. Mendrinos and Rybach L.: Current status of ground source heat pumps and underground thermal energy storage in Europe. *Geothermics*, **32**, (2003), 579-588.

VDI-Richtlinie 4640. Thermische Nutzung des Untergrundes, Teil 2. (Thermal use of the underground, Part 2) Verein Deutscher Ingenieure, VDI-Verlag, Düsseldorf, (2001).

Zheng, C., and Wang, P.P.: MT3DMS: A modular three-dimensional multi-species model for simulation of advection, dispersion and chemical reactions of contaminants in groundwater systems; documentation and user's Guide, Contract Report SERDP-99-1, (1999).